N uptake conditions during summer in the Subantarctic and Polar Frontal Zones of the Australian sector of the Southern Ocean

Marc Elskens, Willy Baeyens, Thierry Cattaldo, and Frank Dehairs
Laboratory for Analytical and Environmental Chemistry, Vrije Universiteit Brussel, Brussels, Belgium

Brian Griffiths
CSIRO Division of Marine Research, Hobart, Tasmania, Australia

Received 2 April 2001; revised 25 October 2001; accepted 22 April 2002; published 5 November 2002.

[1] N uptake data obtained from ^{15}N tracer techniques were surveyed in surface waters of the Subantarctic and Polar Frontal Zones southwest of Tasmania during summer 1998. The N flux rates and *f* ratio were computed using inverse modeling. The approach provides a general framework for the handling of random and systematic variations. Furthermore, factorial experiments based on controlled ammonium additions were used to study the sensitivity of the *f* ratio relative to perturbations of the regenerated nutrient supply. This was achieved in distinct regions: the Subtropical Convergence Zone, the Subantarctic Zone, the Subantarctic Front, and the Polar Frontal Zone. Overall, the stability of the *f* ratio appeared closely related to the availability of both dissolved iron and ammonium. The effect of one factor depended on the level of the other one, and the interaction influenced the *f* ratio patterns. The relationship between *f* ratio and ammonium supplementation ranged from linear to convex curves, with the steepest slopes in water masses rich in dissolved iron and with low ammonium content. The magnitude of this variation may have important ecological and geochemical consequences. Our results suggest that only versatile systems are able to exhibit events of high new production. *INDEX TERMS:* 4203 Oceanography: General: Analytical modeling; 4207 Oceanography: General: Arctic and Antarctic oceanography; 4805 Oceanography: Biological and Chemical: Biogeochemical cycles (1615); 4845 Oceanography: Biological and Chemical: Nutrients and nutrient cycling; 4870 Oceanography: Biological and Chemical: Stable isotopes; *KEYWORDS:* N uptake, f ration, Southern Ocean, isotope dilution model

Citation: Elskens, M., W. Baeyens, T. Cattaldo, F. Dehairs, and B. Griffiths, N uptake conditions during summer in the Subantarctic and Polar Frontal Zones of the Australian sector of the Southern Ocean, *J. Geophys. Res.*, *107*(C11), 3182, doi:10.1029/2001JC000897, 2002.

1. Introduction

[2] Surface waters in the Southern Ocean are generally replete with macronutrients, yet support relatively low new production rates sensu *Dugdale and Goering* [1967]. These high-nitrate, low-chlorophyll (HNLC) regions fail to achieve high new production as a result of low specific nitrate uptake and low phytoplankton biomass [*Dugdale and Wilkerson*, 1992]. While mechanisms believed to set the upper limits to HNLC phytoplankton biomass (both resource and grazer limitations) have received much attention [*Martin et al.*, 1990; *Minas and Minas*, 1992; *de Baar et al.*, 1995; *Boyd et al.*, 1999; *Strom et al.*, 2000], the underlying regulation of the nitrogen assimilation pathway is less known [*Cullen*, 1991]. In the field, there is a striking coincidence between increased ammonium availability and reduced nitrate uptake, emphasizing a regulatory role for ammonium [*Goeyens et al.*, 1991, 1995, 1998b]. Moreover, several investigations provide evidence of a higher iron demand for phytoplankton growth on nitrate than on ammonium [*Price et al.*, 1991, 1994; *Maldonado and Price*, 1996]. Modeling the interdependence of iron and nitrogen, *Armstrong* [1999] suggests a close interaction between iron and ammonium in regulating new production. According to these predictions, a high iron requirement should impede nitrate consumption rates under conditions of iron stress and ammonium availability. As a result, new production should be significantly restrained in nitrate-rich, iron-deficient waters. Because new production carries information about the degree of coupling between processes occurring in the surface and deeper layers [*Eppley and Peterson*, 1979], modeling new production is important to prognostic studies of the global carbon cycle.

[3] Accurate understanding of the related biogeochemical processes requires, however, a critical evaluation of the methods and models used in data processing. Typically, ^{15}N tracer experiments used to assess the importance of new versus regenerated production are based on measurements of concentrations and isotopic ratios. These results are then used in forward models providing N flux rates [*Glibert and*

Copyright 2002 by the American Geophysical Union.
0148-0227/02/2001JC000897$09.00

Capone, 1993; *Legendre and Gosselin*, 1996, and references therein]. Here a different approach is adopted to estimate the N flux rates. The problem is formulated as a constrained optimization and the solution is found iteratively. In contrast to forward models with explicit parameterizations, N flux rates are only constrained by the requirement to fit mass and isotopic balances. The procedure allows assessing model performance, i.e., agreement between measured and predicted values, and provides a statement about result uncertainty. It is commonly referred to as inverse calculation [*Kasibhatla et al.*, 2000].

[4] The aim of this study is twofold: (1) to define and develop criteria for the assessment of N flux rates using appropriate statistical tools, and (2) to analyze the variability of the nitrogen uptake conditions (i.e., the relative importance of new versus regenerated production by the so-called *f* ratio) as a function of ammonium and dissolved iron concentrations, the coupling between uptake and regenerative processes, and the plankton community structure.

[5] This study forms part of the Australian Subantarctic Zone (SAZ) '98 program focusing on the role of the Subantarctic Zone in the Southern Ocean heat and water transports, air-sea gas exchange, primary productivity, ecosystem structure, and carbon export to the deep sea. The data discussed here were gathered during March 1998 (late summer) along a north south transect from 42°S to 55°S and along 142°E.

2. Methods

2.1. The ^{15}N Tracer Experiments

[6] Experiments were designed to investigate the uptake of nitrate, ammonium and urea at ambient levels, and the effect of ammonium additions (0.25, 0.5, and 1μM) on the nitrogen uptake conditions in natural plankton assemblages. Water samples from between 5 and 30 m depth, well within the upper mixed layer, were collected before sunrise with Niskin bottles mounted on a conductivity-temperature-depth (CTD) rosette and dispensed into 2 L acid-cleaned polycarbonate bottles. Unlabeled ammonium in the range of 0–1 μM was added to the bottle sets, and the experiment was started by adding ^{15}N tracers (99 atom %) at final concentrations of 0.5 μM for nitrate, and 0.05 μM for ammonium and urea. Since these amounts of ammonium and urea were dictated more by analytical limitations than by environmental conditions, they increased the concentrations initially to the analytical detection limits, and occasionally exceeded the ambient levels. Bottles were then incubated on deck for 12 hours at natural surface light intensity using a clear Perspex incubator box cooled with flowing surface seawater. Thereafter, particles were concentrated on precombusted glass fiber filters (Whatman GF/F, 25 mm), dried at 50°C, and stored until analysis for isotopic ratios in the laboratory. ^{15}N tracer inoculations, incubations, and filtrations were ordered so as to treat each of the sets in the same way. Subsamples were taken to determine dissolved (nitrate, ammonium, and urea) and particulate nitrogen concentrations at the beginning and the end of the incubation. At all stations, hydrological (temperature, salinity), chemical (nutrient concentrations) and biological parameters (phytoplankton identification and biomass) were measured to complement the basic N incorporation data.

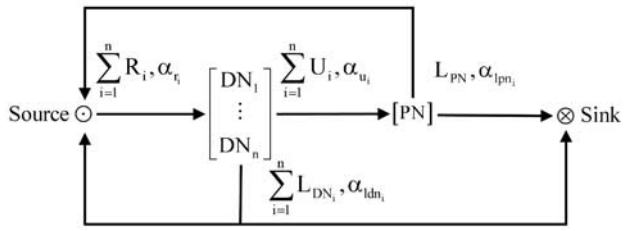

Figure 1. Transfer of ^{15}N into different particulate (PN) and dissolved (DN_i for i = 1…n, where n is the nitrogen substrate) nitrogen pools during an incubation experiment with natural plankton assemblages. Here α_i is the isotopic enrichment (ratio of ^{15}N: $^{14+15}$N) associated with the corresponding nitrogen flux rates: R_i is regeneration, U_i is uptake, L_{DNi} is DN_i loss, and L_{PN} is PN loss.

2.2. Analytical Procedures

[7] Ammonium and urea concentrations were determined manually aboard ship, as described by *Koroleff* [1976] and *Goeyens et al.* [1998a], respectively. Water samples for the determination of nitrate plus nitrite were filtered through cellulose membranes (Millipore type Millex-HA 0.45 μm), stored in polyethylene bottles and frozen until analysis in the home laboratory using a Technicon Autoanalyser method, according to *Hansen and Grasshoff* [1983]. Particulate nitrogen, collected on Whatman GF/F filters after incubation, was converted to dinitrogen by a modified Dumas combustion technique, and ^{15}N isotopic ratio was determined by emission spectrometry using Jasco NIA-1 and N-151 analyzers [*Preston*, 1993]. Particulate organic carbon and nitrogen concentrations were assessed with a Carlo-Erba NA 1500 CN Analyzer, after carbonate elimination in HCl saturated vapor. Quantitative analysis of autotrophic and heterotrophic organisms was based on cell counts and biovolume measurements [*Kopczynska et al.*, 2001].

2.3. The ^{15}N Tracer Models, Differential Equations, and Assumptions

[8] The transfer of ^{15}N tracer into different particulate (PN) and dissolved (DN_i for i = 1…n, where n = the nitrogen substrate) nitrogen pools during an incubation experiment with natural plankton assemblages is outlined in Figure 1. Loss rates from the dissolved and particulate nitrogen pools are source sink processes with respect to the equation for N mass conservation. The source term represents all processes giving rise to a regeneration of the dissolved nitrogen pools during the incubation, such as excretion and release of organic and inorganic nitrogen substrates by the plankton community, bacterial transformations from one nitrogen source to another, e.g., ammonification, nitrification, denitrification. The sink term represents all processes responsible for missing nitrogen within the time span of incubation, such as adsorption of nitrogen on container walls, uptake by bacteria that passed through the GF/F filters used, and breakage of cells containing ^{15}N due to filtration stress. Furthermore, since the isotopic ratios α_{ui} and α_{ldni} are equal to α_{dni}, the isotopic enrichment of the dissolved nitrogen substrate, the differential equations

describing the system for both nitrogen concentrations and isotopic enrichments become:

$$\begin{cases} \partial_t DN_i = R_i - L_{DNi} - U_i \\ \partial_t PN = \sum_{i=1}^{n} U_i - L_{PN} \\ \partial_t \alpha_{dni} = (\alpha_{ri} - \alpha_{dni}) \cdot R_i \cdot DN_i^{-1} \\ \partial_t \alpha_{pni} = \left((\alpha_{dni} - \alpha_{pni}) \cdot U_i + (\alpha_n - \alpha_{pni}) \cdot \sum_{j=1}^{n-1} U_j \right) \cdot PN^{-1} \\ \quad -\left((\alpha_{lpni} - \alpha_{pni}) \cdot L_{PN} \right).PN^{-1} \end{cases} \quad (1)$$

with $i \neq j$ and α_n the natural ^{15}N abundance (0.365 atom %). One of the most widely used forward ^{15}N models can be derived from equation (1) assuming R_i, L_{DNi} and $L_{PN} = 0$. This model is based on the isotopic PN balance at the end of incubation [*Dugdale and Goering*, 1967]:

$$\overline{U}_i = \frac{1}{t} \cdot \int_0^t U_{i,t} dt = \frac{PN_t \cdot (\alpha_{pni,t} - \alpha_n)}{t \cdot (\alpha_{dni,0} - \alpha_n)}, \quad (2)$$

where indices (0, t) denote the initial and final times of the incubation period. Several other rate equations derived from the mass balance approach were suggested [*Dugdale and Wilkerson*, 1986], but *Collos* [1987] showed that equation (2) is more reliable if more than one N source is consumed by the phytoplankton. The simplicity of equation (2) is attractive, but the validity of the underlying assumptions must be ascertained, otherwise estimates of uptake rates might be grossly in error. Improvements to this basic equation were put forward during the two last decades [e.g., *Glibert and Capone*, 1993, and references therein], but these were aimed specifically at correcting for isotope dilution effects due to N regeneration. However, R_i, L_{Dni}, and L_{PN} involve a variety of processes, the importance of which is highly dependent on experimental conditions. With a multivariate model approach such as equation (1), the opportunity arises to gauge these processes while making a minimum number of assumptions. Setting $\alpha_{lpni} = \alpha_{pni}$ and $\alpha_{ri} = \alpha_n$ as will be discussed later, the integration of equation (1) yields:

$$\begin{cases} DN_{i,t} = DN_{i,0} + \left(\overline{R}_i - \overline{L}_{DNi} - \overline{U}_i \right) \cdot t \\ PN_t = PN_0 + \left(\sum_{i=1}^{n} \overline{U}_i - \overline{L}_{PN} \right) \cdot t \\ \alpha_{dni,t} = \alpha_n + (\alpha_{dni,0} - \alpha_n) \cdot \left(1 + \frac{\overline{R}_i - \overline{L}_{DNi} - \overline{U}_i}{DN_{i,0}} \cdot t \right)^{\frac{\overline{R}_i}{\overline{L}_{DNi} + \overline{U}_i - \overline{R}_i}} \\ \alpha_{pni,t} = \frac{\overline{\alpha}_{dni} \cdot \overline{U}_i + \alpha_n \cdot \sum_{j=1}^{n-1} \overline{U}_j}{\sum_{i=1}^{n} \overline{U}_i} \end{cases}$$

$$- \frac{(\overline{\alpha}_{dni} - \alpha_n) \cdot \overline{U}_i}{\sum_{i=1}^{n} \overline{U}_i} \cdot \left(1 + \frac{\sum_{i=1}^{n} \overline{U}_i - \overline{L}_{PN}}{PN_0} \cdot t \right)^{\frac{\sum_{i=1}^{n} \overline{U}_i}{\overline{L}_{PN} - \sum_{i=1}^{n} \overline{U}_i}} \quad (3)$$

with $j \neq i$ and

$$\overline{\alpha}_{dni} = \alpha_n + \frac{(\alpha_{dni,0} - \alpha_n) \cdot DN_{i,0}}{(\overline{U}_i + \overline{L}_{DNi}) \cdot t} \cdot \left(1 - \left(1 + \frac{\overline{R}_i - \overline{L}_{DNi} - \overline{U}_i}{DN_{i,0}} \cdot t \right)^{\frac{\overline{U}_i + \overline{L}_{DNi}}{\overline{U}_i + \overline{L}_{DNi} - \overline{R}_i}} \right) \quad (4)$$

The mass and isotopic balances equation (3) describe a system of $3n + 1$ equations (where n = the number of labeled N substrates), which can be solved for N flux rates using recursive methods.

2.4. Constrained Minimization

[9] Within the context of this study, α_{dni} was not measured (only its initial value $\alpha_{dni,o}$ was calculated), thus resulting in 7 equations (where n = 3 for ammonium, nitrate and urea) with 10 unknowns. Although underidentified, the approach is useful to assess the impact of R_i, L_{DNi} and L_{PN} on the uptake patterns. First, setting

$$\begin{cases} \beta_{dni} = \frac{DN_{i,t} - DN_{i,o}}{t} + \varepsilon_{dni} = \left(\overline{R}_i - \overline{L}_{DNi} - \overline{U}_i \right) + \varepsilon_{dni} \\ \beta_{pn} = \frac{PN_t - PN_o}{t} + \varepsilon_{pn} = \left(\sum_{i=1}^{n} \overline{U}_i - \overline{L}_{PN} \right) + \varepsilon_{pn} \end{cases} \quad (5)$$

where ε are random errors on the data, then by substitution in equation (3), a reduced model form is obtained from the mass balance equations:

$$\alpha_{pni,t} = \frac{\overline{\alpha}_{dni} \cdot \overline{U}_i + \alpha_n \cdot \sum_{j=1}^{2} \overline{U}_j}{\sum_{i=1}^{3} \overline{U}_i} - \frac{(\overline{\alpha}_{dni} - \alpha_n) \cdot \overline{U}_i}{\sum_{i=1}^{3} \overline{U}_i} \cdot \left(1 + \frac{\beta_{pn}}{PN_0} \cdot t \right)^{-\frac{\sum_{i=1}^{3} \overline{U}_i}{\beta_{pn}}}, \quad (6)$$

with $j \neq i$ and

$$\overline{\alpha}_{dni} = \alpha_n + \frac{(\alpha_{dni,0} - \alpha_n) \cdot DN_{i,0}}{(\overline{R}_i - \beta_{dni}) \cdot t} \cdot \left(1 - \left(1 + \frac{\beta_{dni}}{DN_{i,0}} \cdot t \right)^{\frac{\beta_{dni} - \overline{R}_i}{\beta_{dni}}} \right) \quad (7)$$

This allows expressing the isotopic ratios as a function of two endogenous variables only $\overline{U}_i$ and $\overline{R}_i$, β values being obtained from equation (5). The least squares estimates are those values $\overline{U}_i$, $\overline{R}_i$, which fit experimental α_{pni} within 0.1% such that:

$$\begin{cases} \overline{L}_{DNi} = \overline{R}_i - (\beta_{dni} + \overline{U}_i) \\ \overline{L}_{PN} = \sum_{i=1}^{3} \overline{U}_i - \beta_{pn} \\ \overline{U}_i, \overline{R}_i, \overline{L}_{DNi}, \overline{L}_{PN} \geq 0 \end{cases} \quad (8)$$

[10] The fitting was achieved using a quasi-Newton method of iteration [*Chambers*, 1973]. Convergence to the least squares estimates occurred rapidly from any 'reasonable' set of initial estimates, which was obtained, for

example, from solutions provided by equation (2). Because the system is underidentified, there are several combinations of $\overline{U}_i$, $\overline{R}_i$, that can solve equation (6). Therefore, the procedure is repeated in a subroutine until extreme values (min and max) are found for $\overline{U}_i$. These estimates are the lower and upper limits for uptake rates that can be expected considering the constraints introduced in the model calculations. They determine an interval of mathematically possible solutions (solution locus or estimation space) for the data set of interest. To determine which of these solutions are the most likely (S_{min} to S_{max}), C/N uptake ratios were computed using results of ^{14}C incorporation experiments. These ^{14}C results came from small-bottle, short-duration, productivity versus light intensity experiments determining P versus I parameters at the same sampling depths as the nitrogen estimates were performed (B. Griffiths, unpublished data, 2000). Once an "optimal" forecast was obtained, a sensitivity analysis was carried out to assess the impact of systematic and random variations on the final computed results.

2.5. Quantifying Uncertainty

[11] An estimate of the standard deviation of concentrations and isotopic enrichments was calculated using the variability associated with regression lines of calibration standards [*Massart et al.*, 1997]:

$$s_{x^\circ} = \frac{s_{y/x}}{b} \cdot \left(\frac{1}{m} + \frac{1}{n} + \frac{(y^\circ - \overline{y})^2}{b^2 \cdot \sum_{i=1}^{n} (x_i - \overline{x})^2} \right)^{\frac{1}{2}}, \quad (9)$$

where y° is the experimental value from which the concentration or isotopic enrichment x° is to be determined, s_x is the estimated standard deviation of x°, b is the regression coefficient, $s_{y/x}$ is the residual standard deviation, n is the number of calibration points and m is the number of replicates. From equation (9), the pooled estimates of standard deviations for the range of nitrogen concentration and isotopic enrichment encountered in this study are 0.03 μM for $0 \leq [NH_4^+] \leq 0.6$ μM, 0.04 μM for $0 \leq$ [Urea] ≤ 0.2 μM, 0.2 μM for $5.0 \leq [NO_x^-] \leq 25$ μM, 0.05 μM for $0.5 \leq$ [PN] ≤ 1.1 μM, and 0.05 % for $0.5 \leq \alpha_{pni} \leq 3.0$ %. The isotopic enrichments of the dissolved nutrient pools $\alpha_{dni,o}$ were not measured, but calculated with an isotope dilution law. The uncertainty on the final result reflects the random variation in the chemical analysis (9), and is assessed with classical rules for combining standard uncertainties [*Ellison et al.*, 2000]. The pooled estimates of relative standard deviations for the range of $\alpha_{dni,o}$ encountered in this study are 2, 15, and 30% for nitrate, ammonium, and urea pools, respectively.

[12] An estimate of the random variations associated with the N flux rate calculations was computed from the standard uncertainties on β values (5). A number of random deviates on β were generated assuming normal distributions with mean 0 and known variances. Then the N flux rates were recalculated with the new β values as described above, and their statistics evaluated directly. Systematic errors are more difficult to evaluate. The largest potential bias results probably from the fact that natural samples contain varying amounts of detritus nitrogen, the contribution of which cannot easily be determined. Under these conditions, the isotopic enrichment of PN is approximated by:

$$\alpha_{pni} = \alpha_{li} \cdot (1 - \gamma) + \alpha_{nli} \cdot \gamma, \quad (10)$$

where γ is the detritus fraction of PN ($0 \leq \gamma < 1$) and α_{li}, α_{nli} the isotopic enrichments of the living and nonliving fractions, respectively. It can reasonably be assumed that α_{lpni} is proportional to α_{li}, and that the detritus matter has the natural abundance α_n. Hence,

$$\alpha_{lpni} = \alpha_{li} = \frac{\alpha_{pni} - \alpha_n \cdot \gamma}{1 - \gamma} \quad (11)$$

Equation (11) suggests that when $\gamma \sim 0$, α_{lpni} approaches α_{pni}, otherwise $\alpha_{lpni} > \alpha_{pni}$. Another important assumption, made in models used to compute regeneration rates [*Glibert and Capone*, 1993] is that the regenerated nitrogen has the natural abundance, i.e., $\alpha_{ri} = \alpha_n$. The rationale for this assumption arises from the fact that ^{15}N-enriched nitrogen, which is incorporated by phytoplankton, does not immediately find its way into pathways leading to regeneration. Therefore, a time lag can reasonably be expected before any of the enriched ^{15}N will be recycled. Thus, assuming $\alpha_{lpni} = \alpha_{pni}$ and $\alpha_{ri} = \alpha_n$ is an approximation that may bias the estimation of N flux rates by an amount that should be assessed. Expressing α_{lpni} in function of γ (11) and substituting in equation (1), one obtains:

$$\alpha_{pni,t} = \frac{\overline{\alpha}_{dni} \cdot \overline{U}_i + \alpha_n \cdot \left(\sum_{j=1}^{2} \overline{U}_j + \frac{\gamma \cdot \overline{L}_{PN}}{1-\gamma} \right)}{\left(\sum_{i=1}^{3} \overline{U}_i + \frac{\gamma \cdot \overline{L}_{PN}}{1-\gamma} \right)} - \frac{(\overline{\alpha}_{dni} - \alpha_n) \cdot \overline{U}_i}{\left(\sum_{i=1}^{3} \overline{U}_i + \frac{\gamma \cdot \overline{L}_{PN}}{1-\gamma} \right)} \cdot \left(1 + \frac{\beta_{pn}}{PN_0} \cdot t \right)^{-\frac{\sum_{i=1}^{3} \overline{U}_i + \frac{\gamma \cdot \overline{L}_{PN}}{1-\gamma}}{\beta_{pn}}} \quad (12)$$

[13] Equation (12) allows checking the impact of increasing γ on the estimated N flux rates. For each increment of γ, least squares estimates of N flux rates are obtained as described above. To satisfy the fitting criteria, not all values are possible for γ. Therefore, the procedure is applied in an iterative process until a maximum is reached for γ. Three cases must then be considered:

$$\begin{cases} \overline{L}_{PN} = 0 & 0 \leq \gamma \leq \gamma_{max} \quad \alpha_{lpni} = \alpha_{pni} \quad \text{no bias} \\ \overline{L}_{PN} > 0 & \gamma = 0 \quad \alpha_{lpni} = \alpha_{pni} \quad \text{no bias} \\ \overline{L}_{PN} > 0 & 0 < \gamma \leq \gamma_{max} \quad \alpha_{lpni} > \alpha_{pni} \quad \text{bias} \end{cases} \quad (13)$$

The outcome of the sensitivity analysis for systematic and random variations is discussed in the following section (see Figure 4).

3. Results and Discussion

3.1. Model Performance Criteria

[14] N uptake rates were first derived from equation (2). Substituting these rates in equation (3) allowed us to check the agreement between predicted and measured concentrations for both dissolved and particulate nitrogen. In this comparison, the main point of interest is the identification of systematic errors that can occur when the underlying assumptions of equation (2) are not completely valid, as

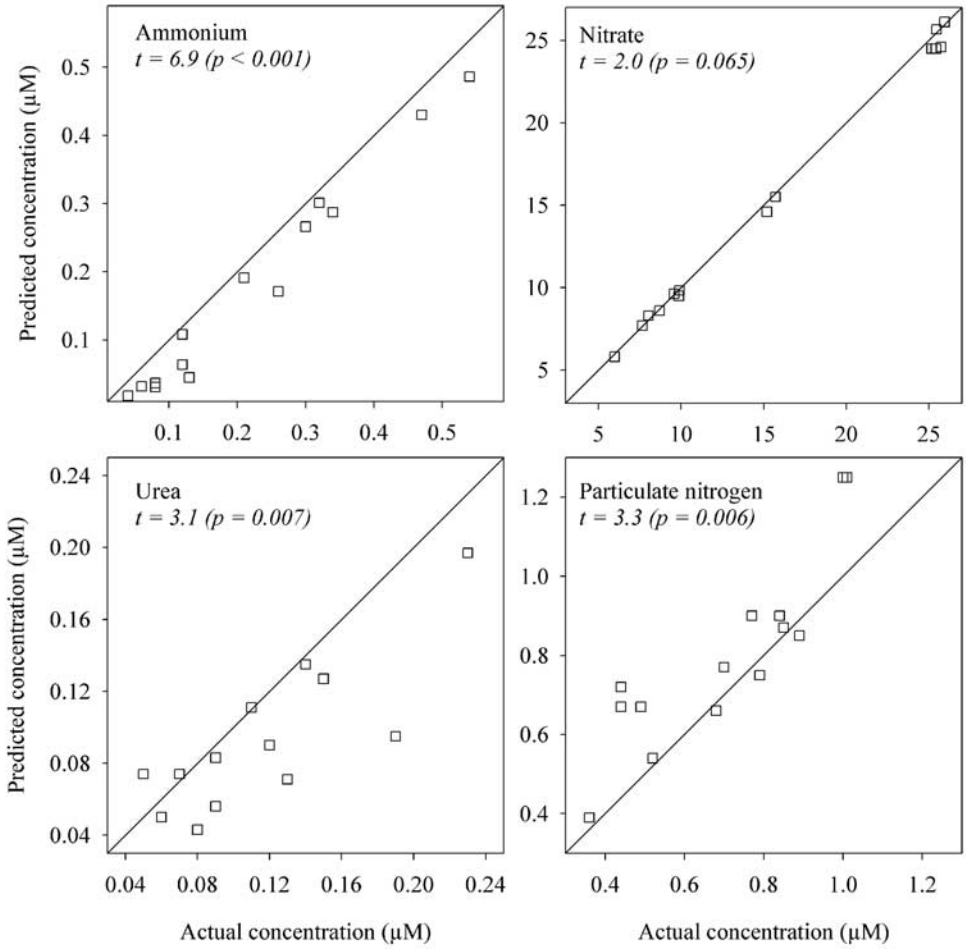

Figure 2. Plots of actual versus predicted nitrogen concentrations. N uptake rates were obtained from equation (2) as described in the text. The solid diagonal depicts the 1:1 relationship. Results of paired *t* test ($t_{crit,\ 95\%} = 2.16$) and related probability are displayed.

would be the case (1) if the net change of the substrate pools with respect to time was the result of consumption and production processes, and (2) if the disappearance of nitrogen from the substrate pools was not balanced by its entrance in particulate matter. As shown in Figure 2, mass balances were not achieved in most uptake experiments. For ammonium and urea, predicted concentrations were consistently lower than observed ones, suggesting that effective regeneration $\overline{R}_i$ and loss rates $\overline{L}_{DNi}$ are such that $\overline{R}_i - \overline{L}_{DNi} > 0$. Conversely, the balance for nitrate was reasonably achieved leading to $\overline{R}_i - \overline{L}_{DNi} \sim 0$. Moreover, field experiments have indicated that nitrification in the upper mixed layer of the studied area was negligible (B. Popp, personal communication, 2000). Finally, the calculated PN concentrations were higher than the observed ones, suggesting that nitrogen was lost from cells, with $\overline{L}_{DNi} > 0$.

[15] Results shown in Figure 2 clearly indicate that the N uptake rates, as obtained from the usual computation formula (2) are significantly biased at the 95% confidence level. Given the available data set, other ^{15}N forward models such as those corrected to account for N regeneration [see *Glibert and Capone*, 1993] could not be applied. In an attempt to improve on this situation, N flux rates were estimated with simulation modeling (6). The procedure starts by determining extreme values for uptake rates (S_{min} and S_{max}) that fit the isotopic enrichment of PN. Because the fitting criteria yield a wide range of possible solutions when the model is underidentified (see section 2), C/N uptake ratios were used to determine which of the solution sets provide the best prognosis. When all the data are compiled into a box plot, S_{min} appears the most likely (Figure 3). The points are randomly and symmetrically distributed around a median of 6.1 slightly below the Redfield C/N ratio of suspended matter. The whiskers representing the tenth to ninetieth percentile range between 3 and 12 in agreement with the variations of C/N ratios usually reported for marine phytoplankton [*Caperon and Meyer*, 1972; *Laws and Wong*, 1978]. A completely different pattern is obtained when considering S_{max}. There is a longer tail at the upper end of the distribution indicating that the points are positively skewed with a median of 0.2. The tenth to ninetieth percentile ranges almost over two orders of magnitude. Thus, while a range of possible solutions has been determined (S_{min} to S_{max}), results in Figure 3 point to S_{min} as the best predictor for the system under study. It allows fitting mass and isotopic balances with a precision of $\leq 0.1\%$ and provides a reason-

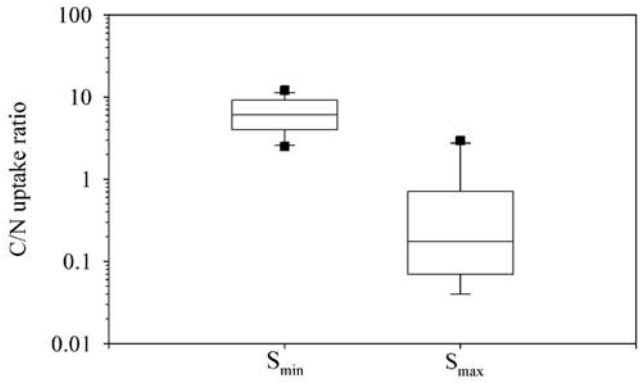

Figure 3. Box and whisker plots of C/N uptake ratio corresponding to lower (S_{min}) and upper (S_{max}) N flux rate estimates. Results of carbon (short-time, P versus I incubations) and nitrogen (corrected for N loss during incubation) incorporation experiments are assumed to represent gross uptake rates. The boxes and the whiskers cover the twenty-fifth to seventy-fifth and the tenth to ninetieth percentiles, respectively. Symbols are outliers.

able forecast given the expected variability on the C/N uptake ratio. However, systematic errors may still remain because of the assumptions underlying the model equations. A sensitivity analysis was carried out to assess the impact of these fluctuations relative to propagated experimental uncertainty. An estimate of random variations on S_{min} was obtained as described in the section 2, and residuals are plotted in Figure 4. The asymmetry about the median results from the fact that N flux rates are approximately lognormal distributed. The evaluation of systematic model errors is more difficult, being chiefly related to γ, the detritus fraction of PN (11). With equation (12), it is possible to evaluate the impact of increasing γ on the estimated N flux rates. The residuals are positively skewed, suggesting that on average S_{min} is underestimated (Figure 4). The situation turns out to be rather satisfactory since the spread associated with

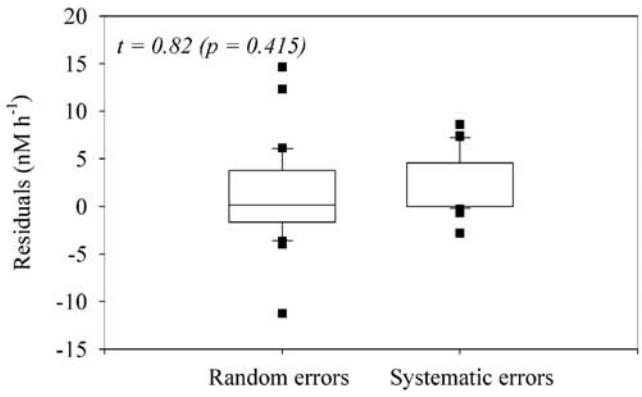

Figure 4. Box and whisker plots of random and systematic variations. The boxes and the whiskers cover the twenty-fifth to seventy-fifth and the tenth to ninetieth percentiles, respectively. Symbols are outliers. Propagation of errors was assessed as described in the section 2. Results of paired *t* test ($t_{crit,\ 95\%}$ = 2.16) and related probability are displayed.

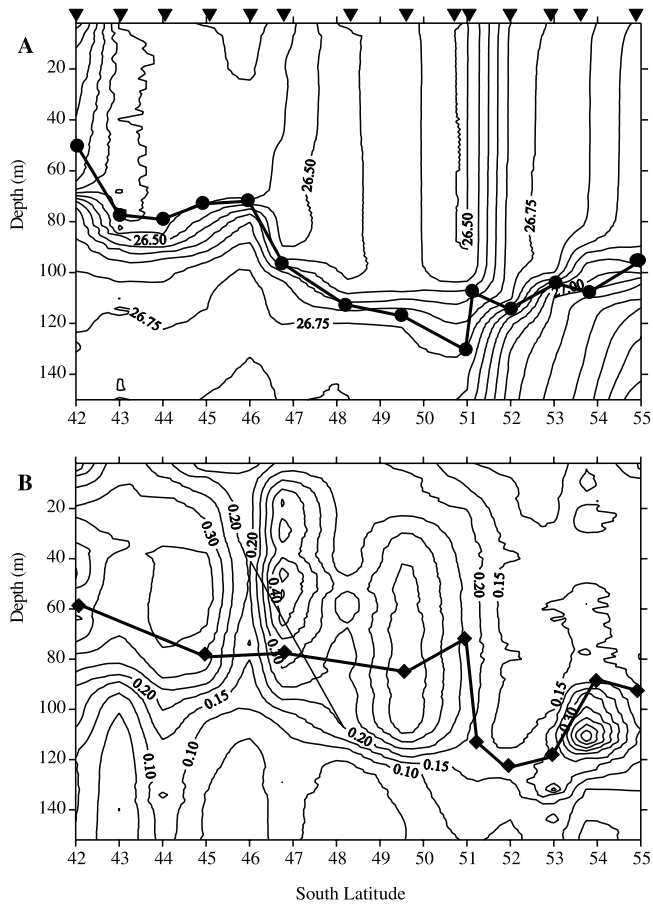

Figure 5. Contours of density and chlorophyll *a* along 142°E. Station locations are shown by solid triangles along the top axis. (a) Contours of density (as Sigma t), with the bottom of the mixed layer indicated by solid circles along 142°E. The bottom of the mixed layer was determined by a change in density of 0.05 units between the surface and depth [*Rintoul and Trull*, 2001]. (b) Contours of chlorophyll a (mg m^{-3}) and 1% light depths (solid diamonds) along 142°E.

systematic model errors is not significantly larger than the one resulting from propagated experimental uncertainty (paired *t* test = 0.82, $p[\leq t_{crit,95\%}] = 0.415$). Hence "true" values for uptake rates are expected to fall within the estimated precision interval [*Ellison et al.*, 2000]. Furthermore, since these uptake rate estimates were corrected for nitrogen loss during incubation, they should be regarded as gross uptake rate [*Bronk et al.*, 1994].

3.2. Study Area

[16] The surveyed section included stations along 141°30′–143°E from the Subtropical Convergence Zone (STCZ) at 42°S to the polar water mass at 55°S, crossing the Subantarctic Front (SAF) near 51°S and the Polar Frontal Zone (PFZ) near 53°S [*Rintoul and Trull*, 2001]. Water of Subantarctic origin (salinity between 34.3 and 34.6 PSU, and temperatures between 9.1 and 11.0°C) was observed between 43° and 49°30′S, but the frontal structure of this water mass is complex and subject to extensive meandering [*Rintoul et al.*, 1997]. A well mixed upper layer deepened progressively from about 50 m at 42°S to 120 m

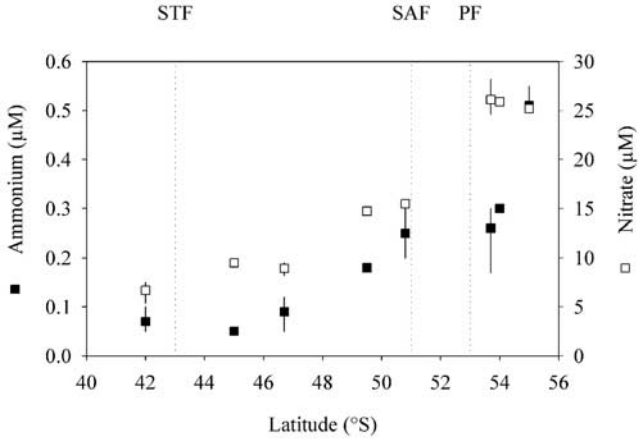

Figure 6. Surface water concentration of nitrate and ammonium (μM). Symbols and bars represent the mean and range of concentration in the average surface stratum (5–30 m). STF = Subtropical Front, SAF = Subantarctic Front, and PF = Polar Front.

at 51°S, while between 51° and 55°S, it shoaled slightly to ~100 m (Figure 5a). Along the entire transect, chlorophyll *a* concentration was distributed homogenously in the surface mixed layer (Figure 5b). Only at 54°S in the PFZ was a subsurface maximum observed at 100 m. Both ammonium and nitrate concentrations in the average surface stratum (5–30 m) increased southwards from ≤0.1 and 6 μM in the STCZ up to 0.55 and 28 μM in the PFZ, respectively (Figure 6). Urea concentrations (≤0.10 up to 0.21 μM) on the contrary did not exhibit significant trends in surface waters with values close to the detection limit of the analytical method.

3.3. N Flux Rates and *f* Ratio

[17] A synopsis of the N uptake patterns in the average surface stratum (5–30 m) is shown in Figure 7. Stations located in the STCZ are characterized by N uptake rates above the mean (all samples) and by low *f* ratios (0.08–0.14). The phytoplankton assemblage was mainly composed of flagellates and dinoflagellates with the latter contributing most to the carbon biomass. It attracted the highest concentration of microzooplankton [*Kopczynska et al.*, 2001]. South of the STCZ, the *f* ratio increased to 0.43–0.51 with total nitrogen uptake rates up to 20 nM h^{-1}. The shift in the nitrogen uptake patterns apparently did not coincide with marked changes in the phytoplankton community structure, but there was evidence for advection of iron at 45°S [*Sedwick et al.*, 1999], perhaps reflecting inputs from Tasmania's southern continental shelf by westward flowing currents [*Rintoul and Sokolov*, 2001]. Between latitudes 47° and 55°S, the *f* ratio oscillated between 0.22 and 0.44 with uptake rates below the mean estimate. Cell densities were lower than in the north and the phytoplankton assemblage showed a southward increasing contribution of diatoms and coccolithophorids to carbon biomass [*Kopczynska et al.*, 2001]. Along the entire transect, the *f* ratio estimates suggest a production system running mainly on regenerated nitrogen, except at 45°–46°S. Overall, ammonium was the dominant nitrogen source used by phytoplankton (47%), followed by nitrate (32%) and urea (21%).

[18] Net changes in the dissolved and particulate nitrogen pools over the incubation period (i.e., the balance between production and consumption processes) are illustrated in Figure 8. A cusum analysis, i.e., the cumulative sum of differences between the observed values and the overall mean, was applied to these data in order to detect patterns of change amongst the randomness [*Massart et al.*, 1997]. This analysis revealed that ammonium demand exceeds regeneration rates at stations north of the Subtropical Front (STF), while ammonium regeneration exceeds demand south of the STF. The pattern is consistent with the observed north-south profile of ammonium in the upper 40m of water column, showing an increase from about 0.1 μM at 42°S to 0.55 μM at 55°S (see Figure 6). Nitrate regeneration is of minor importance, and thus consumption prevails over the whole transect, but with an exceptional event at 45°–46°S. This might possibly reflect the enrichment of surface waters with dissolved iron from a background concentration of 0.1 up to 0.4 nM [*Sedwick et al.*, 1999]. For urea, the data were essentially featureless, except an increase in process variability between latitudes 45°–52°S. For PN, the mean balance of the processes was dramatically modified around 45°–46°S and 51°S. The highest release of nitrogen from PN occurred north of 45°S and coincided with the highest concentration of

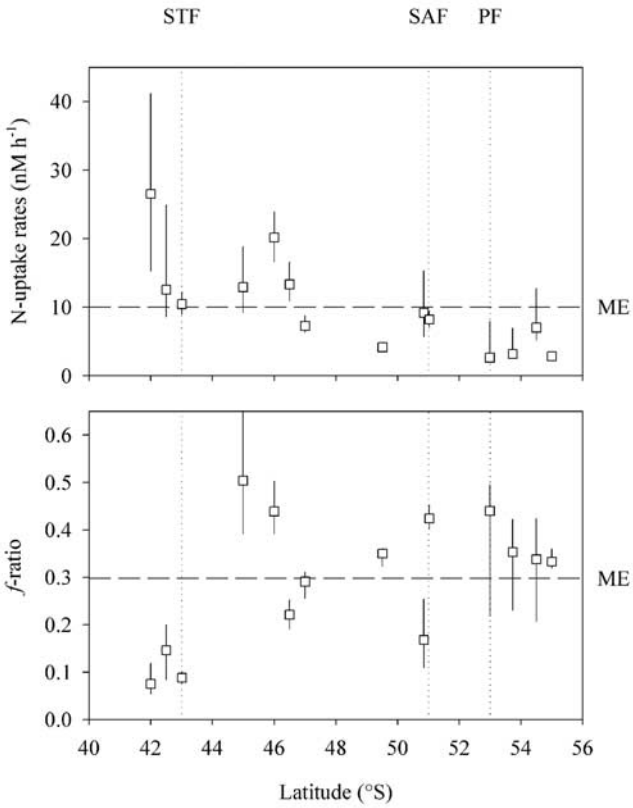

Figure 7. Regional variation of N uptake conditions in surface waters. Bars represent the result uncertainty due to random variations. STF = Subtropical Front, SAF = Subantarctic Front, PF = Polar Front, and ME = mean estimate.

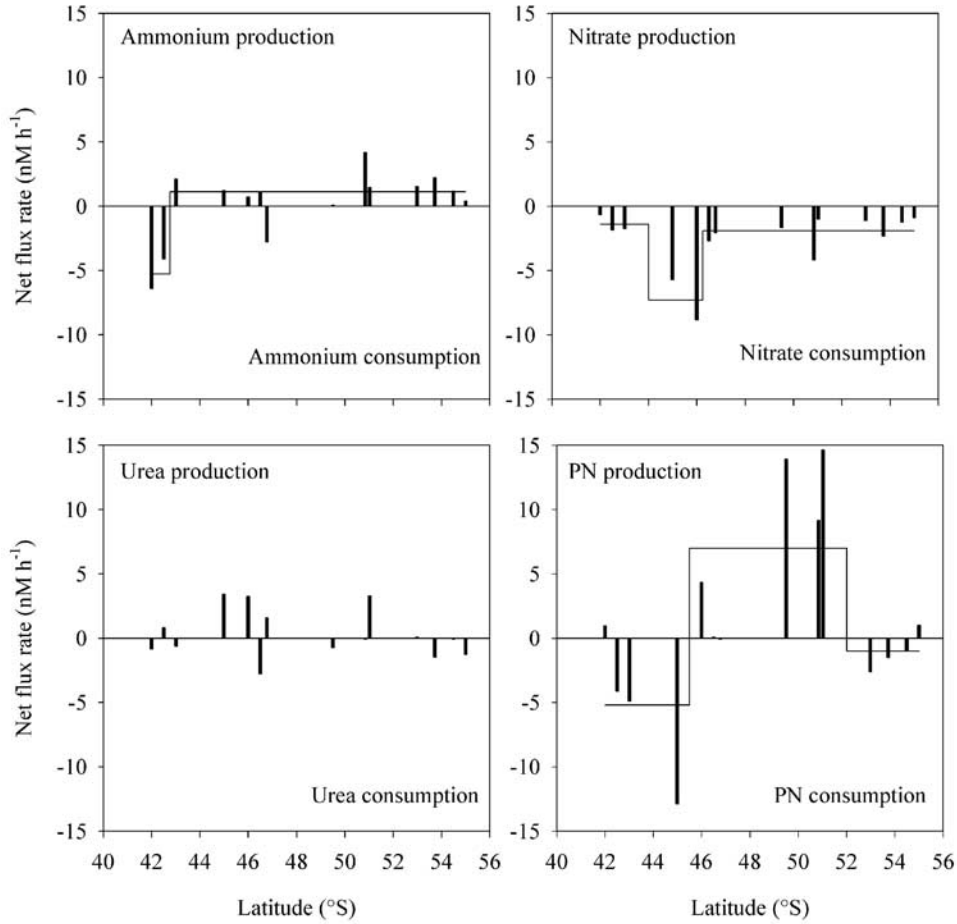

Figure 8. Regional variations of the net N flux rate in surface waters. The solid lines represent the mean balance of the processes as estimated from a cusum analysis (cumulative sum of differences between observed values and the overall mean).

microzooplankton [*Kopczynska et al.*, 2001], thus suggesting that grazing processes were involved.

3.4. Analysis of the Variability in *f* Ratio: Effect of Ammonium

[19] N uptake conditions depend largely on the efficiency of nitrogen regeneration in the surface layer, and on its variation in space and time. Because ammonium is the major regenerated N source, it was used as a trigger agent for investigating the variability in *f* ratio. Ammonium up to 1 μM was added in batch incubation experiments, and N flux rates were computed as described above. Overall, the additions resulted in enhanced ammonium (F = 13.4, $p[\leq F_{crit,95\%}] < 0.001$) and lowered nitrate ($F$ = 25.6, $p[\leq F_{crit,95\%}] < 0.001$) uptake rates, while there was apparently no significant effect on the uptake of urea (F = 0.03, $p[\leq F_{crit,95\%}] = 0.994$) with rates fluctuating randomly within the estimated precision limits. It is important to note that the uptake of nitrate was never totally suppressed even at ammonium concentrations up to 1 μM. The maximum apparent inhibition of nitrate uptake (range 33 to 81%) by 1 μM ammonium is similar to observations by others [e.g., *Dortch*, 1990; *Harrison et al.*, 1996].

[20] Because the observed relationships between *f* ratio and ammonium supplementation were quite variable, ranging from linear to convex curves (Figure 9), they were fitted to rational functions of the form:

$$f = \frac{f^{o} + a \cdot x}{1 + b \cdot x} + \varepsilon_f, \tag{14}$$

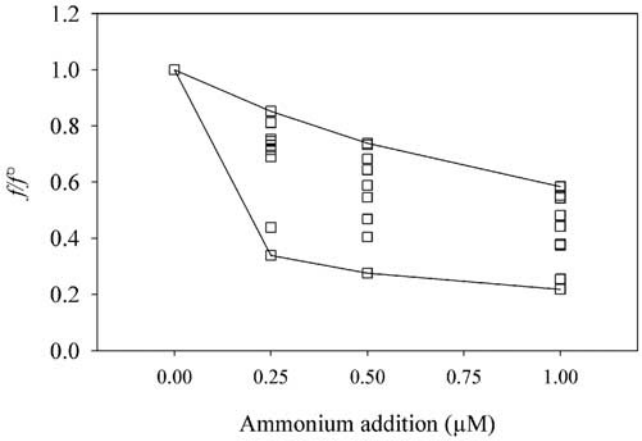

Figure 9. Relative variation of *f* ratio in response to ammonium additions up to 1 μM. Compilation of data obtained for the 142°E section between the STCZ and PFZ.

where f° is the f ratio at ambient concentration, x the amount of ammonium added, a, b the parameters to be estimated, and ε_f the residual term. Such variability in the observed trends is not unusual and has been reported by several authors [*Dortch*, 1990; *Wheeler and Kokkinakis*, 1990; *Armstrong*, 1999, and references therein]. Equation (14) is sufficiently versatile to approximate other mathematical functions, allowing comparisons between various data sets with one model structure. The success of the fitting process was assessed through computation of asymptotic standard errors on parameter estimates and related statistics. Overall, the precision averaged 0.3–8.3 % ($p \leq 0.01$) for f°, 10–19 % ($p \leq 0.01$–0.12) for a, and 5–14 % ($p \leq 0.01$–0.09) for b, p denoting the probability of being wrong in concluding that the parameters were not zero. The sensitivity of the f ratio in the neighborhood of the ambient ammonium concentration was assessed by determining the tangent to the curve (14) at x = 0:

$$y = f^\circ + \left.\frac{df}{dx}\right|_{x=0} \cdot x, \qquad (15)$$

where the slope $df/dx|_{x=0}$ is the first derivative of (14). Slope values were negative and averaged -0.2 ± 0.1, but rose by about one order of magnitude -6 ± 2 at 45°–46°S (Figure 10). Substituting further these values in equation (15) suggests that the f ratio is rather stable throughout, except at 45°–46°S, where it can vary between 0.19 and 0.80 in response to small changes in the ambient ammonium pool ($x = \pm 0.05$ μM).

[21] Dissolved iron concentration in surface water of the SAZ was generally below 1 nM at all stations, but ranged from ≤ 0.1 nM at the southernmost stations up to 0.6 nM at 45°S [*Sedwick et al.*, 1999]. This zone was also characterized by low ambient ammonium (≤ 0.1 μM; Figure 6). A factorial analysis was carried out to test whether the sensitivity of the f ratio was dependent on these factors. Slope values were computed by considering two levels of variations for iron (≤ 0.1 and ≥ 0.4 nM) and ammonium

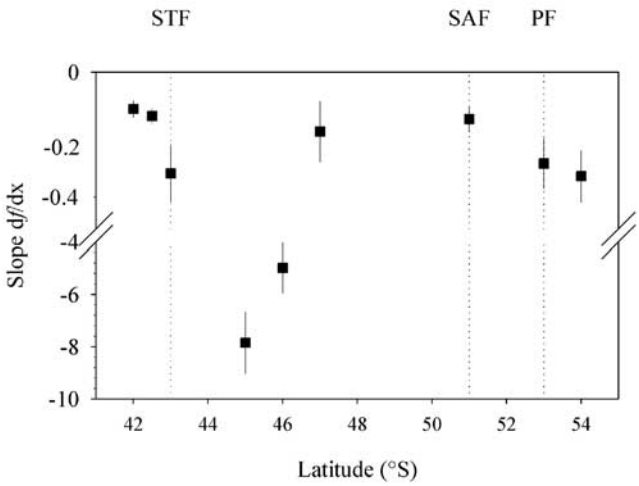

Figure 10. Sensitivity analysis of the f ratio to changes in the ambient ammonium pool. Slope values were determined as described in the text (equation (15)). Bars represent the result uncertainty due to random variations.

Table 1. Anova Analysis of the Effect of Iron and Ammonium on the f Ratio

Source of Variation	Sum of Squares	Degree of Freedom	Mean Squares	F Value	p [$\leq F_{crit,95\%}$]
Single factor ammonium	19.84	1	19.84	19.40	0.012
Single factor iron	20.42	1	20.42	19.97	0.011
Two factor interactions	19.16	1	19.86	18.74	0.012
Residual	4.09	4	1.02		
Total	63.55	7	9.07		

(x up to 0.25 μM). At higher values, i.e., 0.5 and 1 μM, slopes became not significantly different from zero, given uncertainties on parameter estimates. Results in Table 1 suggest close interactions between ammonium and iron in regulating f ratio. This means that the effects of both factors were not merely additive, but in agreement with the model of *Armstrong* [1999].

[22] The various N uptake scenarios may thus be described as follows. In conditions of abundant ambient nitrate and iron limitation, spiking with ammonium has little effect, whether ambient ammonium is low or high. In conditions of enhanced iron availability, abundant ambient nitrate and low ambient ammonium, spiking with ammonium significantly reduced the f ratio, mainly as a result of nitrate uptake inhibition. Therefore, in HNLC areas there may be a seasonal effect on the degree of variation in the f ratio. Early in the growth season, or when there are periodic inputs of nutrients via wind mixing, advection or via atmospheric deposition, the f ratio is quite variable. Later in the growth season, under conditions of iron stress and increased ammonium availability, the f ratio is more steady [see *Goeyens et al.*, 1995, 1998b, and references therein].

4. Conclusions

[23] Most of the "forward ^{15}N models" used to assess N flux rates can be obtained as particular solutions of the system of differential equations corresponding to Figure 1. Care should be taken when applying these models, because they are restricted in their applicability by the validity of the assumptions used to express the parameterizations. Complex reactions such as those outlined in Figure 1 may dramatically influence the quality of the estimates if not properly addressed. The ability of the models to reproduce the data accurately (testing model performance) is, therefore, an important criterion to accept and obtain reliable estimates of N flux rates. The significance test applied here pointed clearly to a rejection of the usual computation formula [*Legendre and Gosselin*, 1996]. Given the available data set, there was little option but to use simulation modeling. The approach based on an iterative optimization procedure yielded simulated data that were generally in good agreement with observations. Although computationally demanding, the technique is powerful and flexible, requiring a small number of assumptions to solve the equations. It provides a much needed strictness in estimating N flux rates, allowing to issue statements about the result uncertainty for both systematic and random variations. However, two caveats of the approach were noted.

1. Given the structure of the data set, there are several local minima for the residuals sum of squares, requiring further model adjustments. From a statistical viewpoint

these adjustments are seldom univocal. Hence any model solution that cannot be proven invalid should be accepted. In the present study for instance, the determination of the isotopic enrichment in the dissolved fraction would have constrained the solution locus significantly.

2. Error analysis of the solution is not straightforward. It was suggested that the largest potential bias on computed nitrogen fluxes results from the presence of varying amounts of detrital nitrogen ($0 \leq \gamma < 1$). Conditions that lead to biased estimates of N flux rates are $\gamma > 0$ and loss of nitrogen from PN during incubation (13). To obtain more information on γ the staining technique developed by *Williams et al.* [1995] could be of interest. Hence, the optimization runs could directly be performed from (12).

[24] Regarding the biogeochemical results, it may be argued that the sensitivity of the *f* ratio is closely controlled by the availability of both dissolved iron and ammonium. Variations in ammonium have their largest impact in situations with high dissolved iron and low ammonium availability. As far as the interaction between ammonium and dissolved iron can be applied throughout HNLC areas, the analysis proposed here should be useful in predicting the level of stability of the production regime. Furthermore, since the *f* ratio carries information about the coupling of processes in the surface and deeper layers, the results of the sensitivity analysis might be significant in forecasting the efficiency of carbon export in the Southern Ocean. Clearly, only versatile systems are able to exhibit events of high new production.

[25] **Acknowledgments.** This research was conducted under grant A4/DD/B11 within the program "Scientific Research on the Antarctic—Phase IV" supported by the Belgian State (The Prime Minister's Services—Scientific, Technical and Cultural Affairs). We thank Tom Trull for his organizational skills and efficient leadership during the SAZ' 98 expedition. We gratefully acknowledge the captain and crew of R/V *Aurora Australis* and the Australian Antarctic Division for assistance in general, and for hospitality aboard the ship.

References

Armstrong, R., An optimization-based model of iron-light-ammonium colimitation of nitrate uptake and phytoplankton growth, *Limnol. Oceanogr.*, *44*, 1436–1446, 1999.

Boyd, P., J. LaRoche, M. Gall, R. Frew, and R. M. L. McKay, Role of iron, light, and silicate in controlling algal biomass in subantarctic waters SE of New Zealand, *J. Geophys. Res.*, *104*, 13,395–13,408, 1999.

Bronk, D. A., P. M. Glibert, and B. B. Ward, Nitrogen uptake, dissolved organic nitrogen release, and new production, *Science*, *265*, 1843–1846, 1994.

Caperon, J., and J. Meyer, Nitrogen-limited growth of marine phytoplankton, I, Change in population characteristics with steady-state growth rate, *Deep Sea Res.*, *19*, 601–618, 1972.

Chambers, J. M., Fitting nonlinear models: Numerical techniques, *Biometrika*, *60*, 1–13, 1973.

Collos, Y., Calculations of ^{15}N uptake rates by phytoplankton assimilating one or several nitrogen sources, *Appl. Radiat. Isot.*, *38*, 275–282, 1987.

Cullen, J. C., Hypotheses to explain high nutrient conditions in the sea, *Limnol. Oceanogr.*, *36*, 1578–1599, 1991.

de Baar, H., J. T. M. de Jong, D. C. E. Bakker, B. M. Loscher, C. Veth, U. Bathmann, and V. Smetacek, Importance of iron for phytoplankton blooms and carbon dioxide drawdown in the Southern Ocean, *Nature*, *373*, 412–415, 1995.

Dortch, Q., The interaction between ammonium and nitrate uptake in phytoplankton, *Mar. Ecol. Prog. Ser.*, *61*, 183–201, 1990.

Dugdale, R. C., and J. J. Goering, Uptake of new and regenerated forms of nitrogen in primary productivity, *Limnol. Oceanogr.*, *12*, 196–206, 1967.

Dugdale, R., and F. Wilkerson, The use of ^{15}N to measure nitrogen uptake in eutrophic oceans: Experimental considerations, *Limnol. Oceanogr.*, *31*, 673–689, 1986.

Dugdale, R., and F. Wilkerson, Nutrient limitation of new production in the sea, in *Primary Productivity and Biogeochemical Cycles in the Sea*, edited by P. G. Falkowski and A. D. Woodhead, pp. 107–122, Plenum, New York, 1992.

Ellison, S. L. R., , M. Rosslein, and A. Williams (Eds.), *EURACHEM/CITAC Guide: Quantifying Uncertainty in Analytical Measurement*, 2nd ed., 120 pp., EURACHEM Meas. Uncertainty Working Group, Teddington, U.K., 2000.

Eppley, R. W., and B. J. Peterson, Particulate organic matter flux and planktonic new production in the deep ocean, *Nature*, *282*, 677–680, 1979.

Glibert, P. M., and D. G. Capone, Mineralization and assimilation in aquatic sediment and wetland systems, in *Nitrogen Isotope Techniques*, edited by R. Knowles and T. H. Blackburn, pp. 243–272, Academic, San Diego, Calif., 1993.

Goeyens, L., F. Sörensson, P. Tréguer, J. Morvan, M. Panouse, and F. Dehairs, Spatiotemporal variability of inorganic nitrogen stocks and assimilatory fluxes in the Scotia-Weddell Confluence area, *Mar. Ecol. Prog. Ser.*, *77*, 7–19, 1991.

Goeyens, L., P. Tréguer, M. E. M. Baumann, W. Baeyens, and F. Dehairs, The leading role of ammonium in the nitrogen uptake regime of Southern Ocean marginal ice zones, *J. Mar. Syst.*, *6*, 345–361, 1995.

Goeyens, L., N. Kindermans, M. Abu Yusuf, and M. Elskens, A room temperature procedure for the manual determination of urea in sea water, *Estuarine Coastal Shelf Sci.*, *47*, 415–418, 1998a.

Goeyens, L., M. Semeneh, M. Elskens, D. Shopova, M. E. M. Baumann, and F. Dehairs, Phytoplanktonic nutrient utilization and nutrient signature in the Southern Ocean, *J. Mar. Syst.*, *17*, 143–158, 1998b.

Hansen, H. P., and K. Grasshoff, Automated chemical analysis, in *Methods of Seawater Analysis*, edited by K. Grasshoff, M. Ehrhardt, and K. Kremling, 2nd ed., pp. 368–376, Verlag Chemie, Weinheim, Germany, 1983.

Harrison, W. G., L. R. Harris, and B. D. Irwin, The kinetics of nitrogen utilization in the oceanic mixed layer: Nitrate and ammonium interactions at nanomolar concentrations, *Limnol. Oceanogr.*, *41*, 16–32, 1996.

Kasibhatla, P., M. Heimann, P. Rayner, N. Mahowald, R. G. Prinn, and D. E. Hartley (Eds.), *Inverse Methods in Global Biogeochemical Cycles*, *Geophys. Monogr. Ser.,* vol. 114, AGU, Washington, D. C., 2000.

Kopczynska, E. E., F. Dehairs, M. Elskens, and S. Wright, Phytoplankton and microzooplankton variability between the Subtropical and Polar Fronts south of Australia: Thriving under regenerative and new production in late summer, *J. Geophy. Res.*, *106*, 31,597–31,609, 2001.

Koroleff, F., Determination of ammonia, in *Methods of Seawater Analysis*, edited by K. Grasshoff, pp. 126–133, Verlag Chemie, Weinheim, Germany, 1976.

Laws, E. A., and D. C. L. Wong, Studies of carbon and nitrogen metabolism by three marine phytoplankton species in nitrate-limited continuous culture, *J. Phycol.*, *14*, 406–416, 1978.

Legendre, L., and M. Gosselin, Estimation of N and C uptake rates by phytoplankton using ^{15}N or ^{13}C: Revisiting the usual computation formulae, *J. Plankton Res.*, *19*, 263–271, 1996.

Maldonado, M. T., and N. M. Price, Influence of N substrate on Fe requirements of marine centric diatoms, *Mar. Ecol. Prog. Ser.*, *141*, 161–172, 1996.

Martin, J. H., R. M. Gordon, and S. E. Fitzwater, Iron in Antarctic waters, *Nature*, *345*, 156–158, 1990.

Massart, D. L., B. G. M. Vandeginste, L. M. C. Buydens, S. De Jong, P. J. Lewi, and J. Smeyers-Verbeke, *Handbook of Chemometrics and Qualimetrics, Part A, Data Handling Sci. Technol.,* vol. 20, 867 pp., Elsevier Sci., New York, 1997.

Minas, H. J., and M. M. Minas, Net community production in "High Nutrient-Low Chlorophyll" waters of the tropical and Antarctic Oceans: Grazing vs. iron hypothesis, *Oceanol. Acta.*, *15*, 145–162, 1992.

Preston, C. M., Optical emission spectrometry, in *Nitrogen Isotope Techniques*, edited by R. Knowles and T. H. Blackburn, pp. 59–87, Academic, San Diego, Calif., 1993.

Price, N. M., L. Anderson, and F. M. M. Morel, Iron and nitrogen nutrition of equatorial Pacific plankton, *Deep Sea Res., Part A*, *38*, 1361–1378, 1991.

Price, N. M., B. A. Ahner, and F. M. M. Morel, The equatorial Pacific Ocean: Grazer controlled phytoplankton population in an iron-limited ecosystem, *Limnol. Oceanogr.*, *39*, 520–534, 1994.

Rintoul, S. R., and S. Sokolov, Baroclinic transport variability of the Antarctic Circumpolar Current south of Australia (WOCE repeat section SR3), *J. Geophys. Res.*, *106*, 2815–2832, 2001.

Rintoul, S. R., and T. W. Trull, Seasonal evolution of the mixed layer in the Subantarctic Zone south of Australia, *J. Geophys. Res.*, *106*, 31,447–31,462, 2001.

Rintoul, S. R., J. R. Donguy, and D. H. Roemmich, Seasonal evolution of upper ocean thermal structure between Tasmania and Antarctica, *Deep Sea Res., Part I*, *44*, 1185–1202, 1997.

Sedwick, P. N., G. R. DiTullio, D. A. Hutchins, P. W. Boyd, F. B. Griffiths, A. C. Crossley, T. W. Trull, and B. Quéguiner, Limitation of algal growth by iron deficiency in the Australian Subantarctic region, *Geophys. Res. Lett.*, *26*, 2865–2868, 1999.

Strom, S. L., C. B. Miller, and B. W. Frost, What sets lower limits to phytoplankton stocks in high-nitrate, low chlorophyll regions of the open ocean?, *Mar. Ecol. Prog. Ser.*, *193*, 19–31, 2000.

Wheeler, P. A., and S. A. Kokkinakis, Ammonium recycling limits nitrate use in the oceanic subarctic Pacific, *Limnol. Oceanogr.*, *35*, 1267–1278, 1990.

Williams, S. C., P. Verity, and T. Beatty, A new staining technique for dual identification of plankton and detritus in seawater, *J. Plankton Res.*, *17*, 2037–2047, 1995.

W. Baeyens, T. Cattaldo, F. Dehairs, and M. Elskens, Analytical Chemistry, Vrije Universiteit Brussel, Pleinlaan 2, B-1050, Brussels, Belgium. (wbaeyens@vub.ac.be; tcattaldo@vub.ac.be; fdehairs@vub.ac.be; melskens@vub.ac.be)

B. Griffiths, CSIRO Division of Marine Research, GPO Box 1538, Hobart, Tasmania, 7001, Australia. (Brian.Griffiths@marine.csiro.au)